



# The effect of inorganic anions on the adsorption of perfluoroalkyl acids to various polymeric anion exchange resins

Lukas Lesmeister<sup>a,\*</sup>, Sarah E. Hale<sup>a</sup>, Michael Merklinger<sup>a</sup>, Harald Horn<sup>b</sup>, Marcel Riegel<sup>a</sup>

<sup>a</sup> TZW: DVGW-Technologiezentrum Wasser (German Water Centre), Karlsruhe Str. 84, Karlsruhe 76139, Germany

<sup>b</sup> Karlsruhe Institute of Technology, Engler-Bunte-Institut, Water Chemistry and Water Technology, Engler-Bunte-Ring 9a, Karlsruhe 76131, Germany

## ARTICLE INFO

### Keywords:

Per- and polyfluoroalkyl substances (PFASs)  
Ultra-short chain  
Perfluorinated carboxylic acids (PFCAs)  
Perfluorinated sulfonic acids (PFASs)  
Weak-base  
Tertiary amine  
Quaternary amine

## ABSTRACT

Anion exchange resins (AERs) are promising adsorbents for removing perfluoroalkyl acids (PFAAs). However, little is known about competitive effects of specific co-solutes at typical drinking water concentrations. Therefore, this study investigated the adsorption of eight PFAAs (1–7 perfluorinated carbons) on three commercial AERs (A111, M600, PSR2Plus) with different functional groups, and examined competitive effects of chloride and sulphate at varying concentrations. Using regression modelling and the stoichiometric breakthrough model, PFAA breakthroughs in fixed-bed filters were simulated, dependent on the concentration of inorganic anions. Generally, the adsorption of PFAAs increased with increasing number and length of alkyl moieties in the functional resin group in the order of dimethylamines (A111) < dimethylethanolamines (M600) < tributylamines (PSR2Plus). Adsorption on PSR2Plus was much less inhibited by the presence of inorganic anions compared to the other resins. Depending on the water matrix and AER used, the relative residual concentration of perfluorocarboxylates as a function of the number of alkyl carbons in the molecule decreased logarithmically, with adjusted  $r^2 \geq 0.93$  and slopes between  $-0.25$  and  $-0.65$  log units per additional carbon. When sulphate and chloride were present simultaneously, sulphate had a stronger inhibitory effect on the adsorption of PFAAs on all resins. Furthermore, a double logarithmic correlation was found between the adsorption of PFAAs and the concentrations of inorganic anions. The results and procedures presented here can be used by water utilities, scientific consultants, and researchers to facilitate the informed selection of AERs for PFAA adsorption and their practical application in fixed-bed filters.

## 1. Introduction

Per- and polyfluoroalkyl substances (PFASs) are widely used in industrial and commercial products [1]. However, due to their high biochemical stability [2] they accumulate in various environmental compartments, including drinking water resources [3–5]. Concerns regarding PFASs are not only related to their persistence [6,7], but also their mobility in the environment [5,8,9], and their toxicity [10]. The increasing awareness of these factors has been driving new regulations

and stricter threshold values. Recently, the recast European Drinking Water Directive introduced a threshold of 100 ng/L for the sum of 20 perfluoroalkyl acids (PFAAs) in drinking water under the name “Sum of PFAS” [11]. This limit includes perfluorocarboxylic acids (PFCAs) with 3–12 perfluorinated alkyl carbons (CF) and perfluorosulfonic acids (PFSAs) with 4–13 CF and therefore, it also covers short-chain PFAAs with 3–7 CF [1,12]. The removal of short-chain (CF  $\leq 7$ ) and ultra-short-chain (CF < 4) PFAAs from contaminated water can be extremely challenging and/or expensive using established treatment methods such as granular activated carbon (GAC) filtration and reverse

**Abbreviations and indices:** 0, initial or at time point zero; AER, Anion exchange resin; avg, Average; B, Breakthrough; b, Slope of linear regression; CAS, Chemical abstracts service number; CF, Perfluorinated alkyl carbons; ci, confidence interval; Cl<sup>-</sup>, Chloride; Eq, Equilibrium; F, Fixed filter bed; GAC, Granular activated carbon; HPLC-MS/MS, High performance liquid chromatography tandem mass spectrometry; inorg.anion, Inorganic anion(s); IS, Internal Standard; m, Mass; NOM, Natural organic matter; PFAAs, Perfluorinated alkyl acids; PFASs, Per- and polyfluorinated alkyl substances; PFBA, Perfluorobutanoic acid; PFBS, Perfluorobutane sulfonic acid; PFCAs, Perfluorinated carboxylic acids; PFHxA, Perfluorohexanoic acid; PFHxS, Perfluorohexane sulfonic acid; PFOA, Perfluorooctanoic acid; PFOS, Perfluorooctane sulfonic acid; PFPeA, Perfluoropentanoic acid; PFPrA, Perfluoropropionic acid; PFSAs, Perfluorinated sulfonic acids; PP, polypropylene; rpm, Rounds per minute; SO<sub>4</sub><sup>2-</sup>, Sulphate; stoic, Stoichiometric; TFAA, Trifluoroacetic acid; TFMS, Trifluoromethane sulfonic acid, theoret.combined effect, Theoretical combined adsorption inhibition effect.

\* Corresponding author.

E-mail address: [lukas.lesmeister@tzw.de](mailto:lukas.lesmeister@tzw.de) (L. Lesmeister).

<https://doi.org/10.1016/j.jece.2024.114871>

Received 5 August 2024; Received in revised form 4 November 2024; Accepted 17 November 2024

Available online 21 November 2024

2213-3437/© 2024 The Authors. Published by Elsevier Ltd. This is an open access article under the CC BY license (<http://creativecommons.org/licenses/by/4.0/>).

### List of symbols used in equations

#### Latin letters

<i>a</i>	Dimensionless coefficient
<i>b</i>	Dimensionless coefficient, slope of linear regression
<i>CF</i>	Perfluorinated carbons
<i>c</i>	mmol/L, Liquid phase molar concentration
<i>K</i>	Adsorption coefficient of a linear isotherm / (L/g)
<i>m</i>	Mass / g
<i>q</i>	Solid phase concentration or loading / (ng/g)
<i>t</i>	Time / days
<i>V</i>	Volume / L

#### Greek letters

$\gamma$	Liquid phase mass concentration / (ng/L)
$\rho$	Density / (g/L)
$\epsilon$	Porosity

osmosis [5,13,14]. Therefore, there is a need for new sustainable and cost-efficient treatment processes.

Previous research on adsorption-based methods has focused on GAC filtration [14–16], biochar [17,18], cyclodextrin-based adsorbents, amorphous aluminium hydroxide, (organo)clays [17,19–21], styrenic  $\beta$ -cyclodextrin polymers [22], and polymeric anion exchange resins (AERs) [23,24]. AERs are particularly promising due to their established use in treating other common water contaminants such as sulphate, chromate, nitrate, chloride, and perchlorate [14], as well as due to their demonstrated effectiveness to treat PFASs for groundwater remediation [24,25]. AERs have a polymer structure, typically styrenic or acrylic, to which positively charged functional groups are attached. These functional groups are balanced by mobile counterions, which can participate in ion exchange (IEX) processes [26–28]. The reported  $pK_a$  values of PFAAs are all  $< 2$ , indicating a negative charge and the ability to take part in anion exchange on AERs at typical environmental pH values [29,30]. PFAA removal by AERs was found to be accompanied by a stoichiometric release (based on charge) of mobile counterions in the exchanger phase, demonstrating that the primary removal mechanism can indeed be attributed to electrostatic interactions [31–33]. However, AERs exhibit greater adsorption affinity and selectivity towards PFAAs with longer alkyl chains [33–35] and with longer alkyl moieties of resin functional groups [34,36], indicating a significant contribution of van der Waals forces and hydrophobic interactions [16,34,37,38]. Similarly, studies have shown that polystyrenic resins adsorb PFAAs better than polyacrylic resins [35,39–42].

To select appropriate AERs for the removal of PFAAs in specific water matrices, a comprehensive understanding of the competitive interactions with other constituents in the matrix is essential. A few studies have investigated the inhibitory effects of natural organic matter (NOM) [35,43–45] and inorganic ions [38,45,46] on the adsorption of PFAAs on AERs. However, drawing comparisons between these studies is challenging due to variations in the type of resin and individual PFASs used. For instance, Deng et al. (2010) observed minimal impacts on the adsorption of perfluorooctane sulfonic acid (PFOS) on a strongly basic polyacrylic resin with an increase in sulphate concentration from 0 to 1 mmol/L, while a decrease of up to 27 % in PFOS adsorption was observed for a weakly basic polyacrylic resin under similar conditions. [47]. Maimaiti et al. (2018) reported only a 10 % reduction in the adsorption of perfluorohexane sulfonic acid (PFHxS) on a polystyrenic strongly basic type II resin at high concentrations of 50 mmol/L of various inorganic ions [33]. Yang et al. (2018) found significant decreases in perfluorooctanoic acid (PFOA) removal by a strongly basic polyacrylic resin upon the addition of 1 meq/L of chloride, hydrogen carbonate, carbonate or sulphate ions [46]. There is currently a research

gap related to the impact of inorganic ions on the adsorption of short-chain PFAAs [23]. In this context, only Tan et al. (2023) have conducted an extensive investigation where four different AERs and ten PFASs were tested, though relatively high PFAS concentrations (200  $\mu\text{g/L}$ ) were used and the inorganic ion concentrations were comparatively low (5 mg/L) compared to typical drinking water conditions [11,45]. Consequently, there is a lack of information about the competitive effects of various inorganic anions on the adsorption of short-chain PFAAs at concentrations typical of drinking water, for one or both types of chemicals.

To address this research gap, the present study investigated the adsorption behaviour of eight PFAAs (CF1–7) onto three commercially available AERs (A111, M600, PSR2Plus) with various functional groups and also considered the competitive effects of chloride and sulphate at typical drinking water concentrations. The experimental conditions were selected to facilitate a comprehensive analysis of the adsorption of CF2–4 PFCAs onto the weakly basic resin A111, while concurrently comparing their adsorption behaviour with other PFAAs and AERs exhibiting different characteristics.

Furthermore, the relationship between the adsorption of PFAAs to a particular AER and the concentration of specific inorganic anions in the bulk solution was mathematically described, progressing beyond previous studies [33,45–47]. It is hypothesized that insights obtained from batch experiments to describe such a relationship can be leveraged to forecast the suitability of a specific AER for the removal of PFAAs in fixed-bed filters. Therefore, the present study derived a mathematical equation to describe the relative residual PFAA concentration,  $\gamma/\gamma_0$ , after treatment with a specific AER as a function of the chloride and sulphate concentrations. The equation was subsequently used to ascertain maximum throughputs in fixed-bed filters to the stoichiometric breakthrough for a range of PFAAs when a specific AER was used. Indeed, the accuracy of adsorption equilibrium results to predict the performance in fixed bed filters is a simplistic approach and thus has its limitations. However, providing a value for the breakthrough relates the results to practical applications and thus improves their meaning for decision makers. Hence, the overall objective of the work was to provide a tool to facilitate the (pre-)selection of suitable AERs for the removal of PFASs from drinking water, particularly in the early stages of material evaluation, prior to more in-depth but also more elaborate column studies.

## 2. Materials and methods

### 2.1. Perfluoroalkyl acids (PFAAs)

Table 1 lists the analytical grade PFAA standards and the isotopically labelled internal standards (ISs) used in the experiments. A standard solution containing 0.1 g/L per compound was prepared in ultrapure water ( $> 18.2 \text{ M}\Omega$  at  $25^\circ\text{C}$ , filtered with an Arium® Pro, Sartorius AG, Göttingen, Germany) and used for the experiments and analytical procedures.

### 2.2. Anion exchange resins (AERs)

All three selected resins (Table 2) had a polystyrene-based backbone structure but differed in their alkyl amine moieties of their functional groups. These resins have previously demonstrated promising results for the adsorption of PFAAs and/or regeneration [48]. Purolite A111 (Purolite, United States) is a weakly basic AER with tertiary amine functional groups only. Lewatit MonoPlus M600 (LANXESS, Germany) is a type II strongly basic AER with dimethylethanolamine functional groups. AmberLite PSR2Plus (DuPont de Nemours, United States) is a strongly basic AER specifically designed for the removal of PFASs. For clarity, the AERs will be referred to without their trade names for the remainder of this article.

Before the resins were used in the batch experiments, they were first

**Table 1**  
PFAAs and isotopically labelled internal standards used in this study.

Abbreviation	Substance	Standard (purity)	CAS	Internal standard
TFAA	trifluoroacetic acid	sodium trifluoroacetate, ( $\geq 99.0\%$ ) <sup>a</sup>	2923-18-4	sodium trifluoroacetate-13C <sub>2</sub> <sup>c</sup>
PFPrA	perfluoropropanoic acid	pentafluoropropionic acid (97 %) <sup>b</sup>	422-64-0	perfluoropropanoic acid-13C <sub>3</sub> <sup>d</sup>
PFBA	perfluorobutanoic acid	perfluorobutanoic acid, (99 %) <sup>b</sup>	375-22-4	perfluoro-n-[1,2,3,4-13C4]butanoic acid <sup>c</sup>
PFPeA	perfluoropentanoic acid	n-perfluoropentanoic acid (98 %) <sup>b</sup>	2706-90-3	perfluoro-n-[1,2,3,4,5-13C5]pentanoic acid <sup>c</sup>
PFHxA	perfluorohexanoic acid	perfluorohexanoic acid (98 %) <sup>b</sup>	307-24-4	perfluoro-n-[1,2-13C2]hexanoic acid <sup>c</sup>
PFOA	perfluorooctanoic acid	perfluorooctanoic acid (95 %) <sup>b</sup>	335-67-1	perfluoro-n-[1,2,3,4-13C4]octanoic acid <sup>c</sup>
TFMS	trifluoromethanesulfonic acid	lithium trifluoromethane-sulfonate (99.995 %) <sup>a</sup>	33454-82-9	sodium perfluoro-1-[2,3,4-13C3]butanesulfonate <sup>c</sup>
PFBS	perfluorobutanesulfonic acid	potassium nonafluoro-1-butanesulfonate (98 %) <sup>a</sup>	29420-49-3	sodium perfluoro-1-[2,3,4-13C3]butanesulfonate <sup>c</sup>

<sup>a</sup> Sigma-Aldrich (Steinheim, Germany)<sup>b</sup> ABCR GmbH (Karlsruhe, Germany)<sup>c</sup> Wellington Laboratories (Guelph, Ontario, Canada)<sup>d</sup> Cambridge Isotope Laboratories, Inc. (Tewksbury, MA, United States)**Table 2**  
Characteristics of tested anion exchange resins.

Name	Polymer Matrix	Pore Structure	Functional Group	Basicity	Ionic Form	Density (as shipped) / (kg/L)	Total Exchange Capacity / (eq/L)
A111	Styrenic	Macroporous	Dimethylamine	Weak	Free base	0.66	1.7
M600	Styrenic	Gel	Dimethylethanolamine	Strong	Chloride	0.68	1.3
PSR2 Plus	Styrenic	Gel	Tri-n-butyl amine	Strong	Chloride	0.69	$\geq 0.7$

Information from manufacturers' data sheets, see [supplementary information](#) in Appendix 1.

washed and conditioned (see details in Section A.1 of Appendix A), soaked in demineralized water ( $\leq 1 \mu\text{S}/\text{cm}$ ) and centrifuged at 1300 g for 20 min at 20°C to bring them to a uniformly defined state. The AERs were tested in the same ionic form in which they were supplied, i. e. the free base form for the weakly basic AER and the chloride form for the two strongly basic AERs. A111 was tested in its free base form as recent studies have shown that weakly basic AERs can perform well in PFAS adsorption at neutral and acidic pH without first being converted to another form with a specific counterion [42,48], which would be advantages for potential applications in which the resin is frequently regenerated with a caustic solution.

### 2.3. Batch experiments

The present study aimed to explore the effect of sulphate ( $\text{SO}_4^{2-}$ ) and chloride ( $\text{Cl}^-$ ) on the adsorption of PFAAs on different AERs. Test solutions were prepared to encompass a range of concentrations (0.5 mM to 3.8 mM) of sodium chloride ( $\geq 99.5\%$ , Merck, Germany) and sodium sulphate ( $\geq 99\%$ , p.a., Carl Roth, Germany), as detailed in Table 3. As such, the concentration covered a range typical of drinking water ( $< 250 \text{ mg}/\text{L}$  [11]) and the lower range of membrane concentrates (highest concentrations) which meant that typical and also worst-case drinking water conditions could be tested. The pH of each solution was adjusted

to  $7.0 \pm 0.1$  using 0.1 M NaOH obtained from Merck, Germany. For each anion, triplicate sets of four different concentrations were prepared in deionized water. Furthermore, identical concentrations of sulphate and chloride were incorporated into a third set of tests to examine the combined effect of both anions. A set with pure deionized water was also prepared as a reference for adsorption without competition from inorganic anions. Prior to the experiments, the deionized water used was analysed for PFAAs, chloride and sulphate. The results of the deionized water analysis did not show any contamination since all parameters were below the respective limits of quantification (LOQs) (Table A.1). Additionally, for three of the treatment series, batches without resin were included as a control that showed that adsorption in the bottles without resin was negligible.

Since the primary interaction force between PFAAs and inorganic anions is the electrostatic repulsion of their negative charges, where monovalent chloride has one negative charge and bivalent sulphate has two, comparing their effects solely based on the molar concentration is difficult from a mechanistic perspective. For this reason, the individual concentrations in each of the three series (chloride, sulphate, both) were selected so that a comparison of the effects based on charge equivalents and electric conductivity  $\kappa$  was also possible (bold italic groups in Table 3). The electric conductivity at 25°C was determined using a TetraCon 325 conductivity measuring cell from WTW, Weilheim,

**Table 3**  
Chloride and sulphate concentrations, charge equivalents and electric conductivity in batch experimental groups.

Anions	[NaCl] / (mmol/L)	[Na <sub>2</sub> SO <sub>4</sub> ] / (mmol/L)	[Cl <sup>-</sup> ] / (mg/L)	[SO <sub>4</sub> <sup>2-</sup> ] / (mg/L)	Total Negative Charge / (meq/L)	$\kappa$ / ( $\mu\text{S}/\text{cm}$ )
Chloride	0.5	-	18	-	0.5	63
	1.3	-	46	-	1.3	163
	1.9	-	68	-	1.9	243
	3.8	-	136	-	<b>3.8</b>	<b>454</b>
Sulphate	-	0.5	-	48	1.0	130
	-	1.3	-	124	2.6	335
	-	1.9	-	178	<b>3.7</b>	<b>453</b>
	-	3.8	-	369	7.7	1000
Both simultaneously	0.5	0.5	17	47	1.5	190
	1.3	1.3	46	124	<b>3.9</b>	<b>452</b>
	1.9	1.9	68	185	5.7	743
	3.8	3.8	136	369	11.5	1480
deionized water	$< 0.03$	$< 0.01$	$< 1$	$< 1$	$< 0.05$	$\leq 1$

 $\kappa$  = electric conductivity at 25°C, bold values show batches with comparable negative charge equivalents and  $\kappa$ .

Germany.

Batch adsorption experiments were conducted in pyrolyzed 250 mL glass bottles. Each bottle was filled with 200 mL of the respective test solution and spiked with PFAAs. It was important to obtain comparable equilibrium concentrations of the PFAAs for all AERs for the simulation of similar adsorption conditions in fixed-bed filters and the calculation of isotherm parameters. For this reason, higher initial PFAA mass concentrations,  $\gamma_0$ , were spiked into the bottles containing PSR2Plus (35  $\mu\text{g/L}$ ) than into the bottles containing A111 or M600 (4  $\mu\text{g/L}$ ), because a higher adsorption capacity was anticipated for PSR2Plus, given that it was a PFAS-specific resin. The dosed concentrations of PFAAs were determined based on preliminary experiments and conditions that were deemed best suited for investigating the adsorption of CF2–4 PFCAs onto A111.

Following PFAA spiking, the bottles were shaken horizontally on a laboratory shaker (GFL Orbital Shaker 3019, GFL, Germany) for 5 min and mixed before aliquoting 10 mL-samples to determine the initial PFAA concentrations. After the addition of 0.1 g of centrifuged AER (preparation details outlined in Section 2.2), the bottles were shaken at 180 rpm for at least 60 h at ambient laboratory temperature to ensure adsorption equilibrium (see results of preliminary equilibrium experiment in Fig. A.1, Section A.3). The mixing speed mirrors that of previous studies [49] and was selected so that the particles of all three AERs were uniformly and well suspended in every bottle to minimize external mass transfer resistances. Following this, samples were taken for PFAA analysis. Without further pre-treatment, the samples were stored at 4 °C in polypropylene (PP) vials until analysis. All batches were prepared in triplicate.

#### 2.4. Analysis

PFAAs were analysed using high performance liquid chromatography tandem mass spectrometry (HPLC-MS/MS) using direct injection from PP vials with minimal preparation. Sampling vials contained a total volume of 1 mL sample, diluted with ultrapure water if necessary, and 10  $\mu\text{L}$  IS standard solution (0.1 mg/L in methanol). Substance specific ISs were implemented for the correction of matrix effects for all PFAAs except for trifluoromethane sulfonic acid (TFMS), which was interpreted with the IS for PFBS (Table 1). An Agilent 1290 Infinity HPLC system (Waldbronn, Germany) and an AB Sciex 6500+ triple quadrupole mass spectrometer (Framingham, MA, United States) with electrospray ionization in negative ionization mode and multiple reaction monitoring were used. A Dionex IonPac™ AS17-C RFICTM 2 × 250 mm, with a Dionex IonPac™ AG17-C RFICTM 2 × 50 mm guard column, Thermo Fisher Scientific (Darmstadt, Germany), was used for chromatographic separation. Injection volume, flow and temperature were 100  $\mu\text{L}$ , 0.28 mL/min and 30°C ± 2°C, respectively. The solvents used were 20 % methanol in ultrapure water plus 100 mM  $\text{NH}_4\text{HCO}_3$  and 100 % methanol. Methanol was purchased from Promochem (Wesel, Germany) and  $\text{NH}_4\text{HCO}_3$  from Sigma-Aldrich (Steinheim, Germany). The solvent gradient per run, retention times, ion masses and MS/MS parameters are given in Section A.4 of Appendix A. LOQs were determined according to DIN 32645:2008–11 [50] and were 10 ng/L in the undiluted samples for all PFAAs. Calibration was done with 15 points between 5 ng/L and 5000 ng/L.

The chloride and sulphate concentration was determined according to DIN EN ISO 10304–1:2009–07 [51] using an ICS1100 ion chromatograph with an IonPac AS 22 column and AG 22 guard column (Thermo Fisher Scientific, Darmstadt). The LOQs were 1.0 mg/l for chloride and sulphate.

### 3. Theory and calculation

#### 3.1. Determination of adsorption performance

Adsorption performance was expressed as the residual concentra-

tion,  $\gamma$ , relative to the initial concentration,  $\gamma_0$ , as  $\gamma/\gamma_0$ . Lower  $\gamma/\gamma_0$  values indicate better adsorption performance. Inhibitory effects of different anions were determined by comparing  $\gamma/\gamma_0$  in deionized water with those in other batches. However, the inhibition caused by chloride or sulphate individually was likely less than when both were present together, as these anions also compete for adsorption sites on the AERs. To test this, the theoretical combined inhibition was calculated by summing the separate inhibitions from chloride and sulphate (Eq. (1)) and comparing it to the inhibition in the series with both anions, the actual combined inhibition. When the theoretical combined effect suggested 100 % inhibition (no adsorption),  $\gamma/\gamma_0$  was assumed to be 1.

$$(\gamma/\gamma_0)_{\text{theoret. combined effect}} = (\gamma/\gamma_0)_{\text{chloride}} + (\gamma/\gamma_0)_{\text{sulphate}} - 2 * (\gamma/\gamma_0)_{\text{demineralized water}} \quad (1)$$

To further characterize the relationship between  $\gamma/\gamma_0$  and the inorganic anion concentration  $c_{\text{inorg. anion}}$ , this ratio was expressed as a function of  $c_{\text{inorg. anion}}$  in Eq. (2), where  $c_{\text{inorg. anion}}$  is in mmol/L,  $\log(a)$  is the intercept and  $b$  is the slope of a linear regression.

$$\log(\gamma/\gamma_0) = \log(a) + b * \log(c_{\text{inorg. anion}}) \quad (2)$$

Regression analysis was performed using R [52]. If the adjusted coefficient of determination,  $r_{\text{adj}}^2$ , was below 0.8 or the slope's p-value was not significant ( $p > 0.05$ ), the double-logarithmic model was discarded, as marked in the figures and tables.

For PFCAs, the relationship between  $\gamma/\gamma_0$  and CF in the PFAA molecule were expressed by Eq. (3).

$$\log(\gamma/\gamma_0) = \text{intercept} + \text{slope} * CF \quad (3)$$

Additionally, the equilibrium concentration in the bulk solution,  $\gamma_{\text{eq}}$ , and the loading of the AER,  $q_{\text{eq}}$ , were obtained from the batch experiments by measuring  $\gamma_{\text{eq}}$  directly and calculating  $q_{\text{eq}}$  using Eq. (4).

$$q_{\text{eq}} = (V_L/m_{\text{AER}}) * (\gamma_0 - \gamma_{\text{eq}}) \quad (4)$$

Here,  $V_L$  is the liquid volume,  $m_{\text{AER}}$  is the AER mass, and  $\gamma_0$  is the initial PFAA mass concentration. The units applied for these quantities are given in the List of symbols used in equations.

#### 3.2. Prediction of PFAA breakthroughs

Breakthrough refers to the point at which the effluent concentration of a substance in a fixed-bed filter reaches a threshold, signaling that the filter is no longer effectively removing it. The stoichiometric breakthrough, based on Sontheimer et al., 1985 [53], was applied here to estimate breakthroughs using equilibrium data from the batch experiments only. This model assumes immediate adsorption equilibrium, pure plug flow conditions, as well as favorable adsorption conditions, and can be calculated using Eq. (5) (see Section A.7 for a more detailed derivation).

$$V_{\text{stoic}} = \frac{q_{\text{eq}}}{\gamma_{\text{qe}}} * \rho_F * V_F \quad (5)$$

To compare breakthroughs at identical influent concentrations, mean values from the triplicate batch experiments were used to fit a linear isotherm for each PFAA, as shown in Eq. (6). This assumption was justified with the low concentrations of PFAAs compared to other matrix compounds, allowing them to be considered as trace species [27] (more information in Section A.7).

$$q_{\text{eq}} = K\gamma_{\text{eq}} \quad (6)$$

Solving for the adsorption coefficient,  $K$ , and inserting it into Eq. (5) gives:

$$V_{\text{stoic}} = K * \rho_F * V_F \quad (7)$$

To normalize  $V_{\text{stoic}}$  and make it independent of  $V_F$ , it is divided by  $V_F$ ,

yielding bed volumes (BV) until breakthrough,  $V_B$ , as shown in Eq. (8):

$$V_B = K * \rho_F \quad (8)$$

In the same way as described for  $\gamma/\gamma_0$  and  $c_{inorg,anion}$ , the relationship between  $V_B$  and  $c_{inorg,anion}$  was described using a double-logarithmic model.

### 3.3. Data evaluation

Grubbs tests for outliers were conducted on the  $\gamma_{eq}$  triplicates (p-values of  $\leq 0.1$  due to the low test power with triplicates). Means and standard deviations were calculated for  $\gamma_0$ ,  $\gamma_{eq}$  and  $q_{eq}$  where possible. If an outlier was removed or one value was below the LOQ, calculations were based on the remaining duplicates. Single values were used in further calculations if no duplicates were available, as values below the LOQ were not quantified. The relative standard deviation (RSD) was used to assess reproducibility, with values  $\leq 0.2$  or  $\leq 20\%$  deemed acceptable.

For further analysis, paired Wilcoxon rank sum tests with Bonferroni correction were applied for each AER to compare the effects of different anions (chloride, sulphate, both). AER performance was also compared for each anion group. For batches with similar conductivity ( $\chi \approx 450 \mu\text{S}/\text{cm}$ ), t-tests with Bonferroni correction were performed, following Shapiro-Wilk tests for normality and Bartlett's tests for variance homogeneity.

## 4. Results and discussion

### 4.1. Data evaluation

The raw data from the PFAA measurements can be found in Appendix B in the document called Supplementary\_Information\_2.xlsx in the data sheet called "rawdata". Cases in which Grubbs tests on  $\gamma_{eq}$  lead to the removal of outliers are presented in Table A.4. In two cases (A111, PFOA, 1.9 mM  $\text{Cl}^-$  and A111, PFBS, 0.5 mM  $\text{Cl}^-$ ), only one measurement value was available. For the three control batches without resins, results showed that adsorption was negligible with  $\gamma/\gamma_0$  between 95 % and 108 % (Table A.5). Based on the 95th percentiles for the RSDs of  $\gamma_0$ ,  $\gamma_{eq}$  and  $q_{eq}$  (0.08, 0.15, and 0.14, respectively), more than 95 % of the data met the inclusion criteria (equal or less than 20 %). Consequently, to maintain a comprehensive overview of all results, except for the Grubbs outliers, no data was excluded from the analysis. A brief discussion of some comparably high RSDs is included in Appendix A (Section A.5). The results of further data processing and statistical analysis are included in the respective sections in Appendix A.

### 4.2. Adsorption inhibition contingent on inorganic ion concentrations

#### 4.2.1. Separate effects of sulphate and chloride

Compared to the adsorption in deionized water, the adsorption of PFAAs onto the AERs was inhibited by chloride and sulphate ions (Fig. 1). Sulphate exerted a significantly greater inhibitory effect than chloride for the CF1–5 PFCAs and all AERs as well as for TFMS using

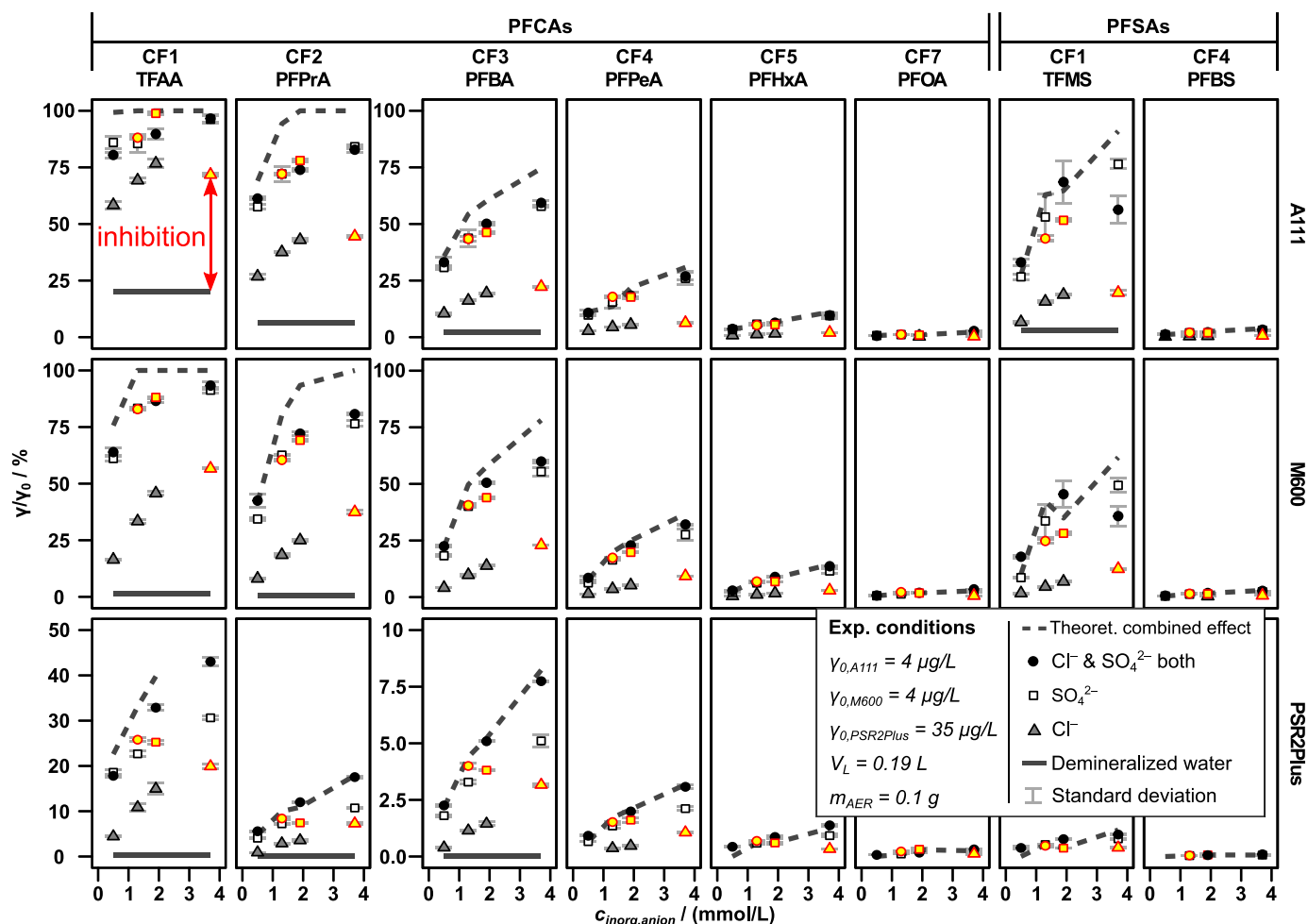


Fig. 1. Relative residual PFAA concentrations,  $\gamma/\gamma_0$ , at various inorganic anion concentrations,  $c_{inorg,anion}$ , using three different AERs. Batch groups for comparison based on charge equivalents ( $\sim 3.8 \text{ meq}/\text{L}$ ) are highlighted in red framed yellow. Note different scales on y-axis.

A111 and M600 ( $p < 0.05$ , Table A.6). This was also true when the inhibition was compared between the batches with and without sulphate containing different anion concentrations but an equal amount of negative charge equivalents (red framed yellow in Fig. 1,  $p < 0.05$ , sheet "el.cond.450\_stats" in Supplementary\_Information\_2.xlsx), with very few exceptions. These results are indicating a preference for bivalent anions such as sulphate over monovalent ones such as chloride by all tested AERs. In contrast to the inorganic chloride, where electrostatic interaction is the only force of interaction with AER active sites, the adsorption of organic PFAAs is supported by other forces including hydrophobic interaction and van der Waals forces [16,34,37,38], facilitating the adsorption of PFAAs compared to sulphate. However, the greater selectivity towards divalent anions thus also causes the adsorption of monovalent PFAA anions to be stronger inhibited by divalent sulphate than monovalent chloride. One explanation uses Le Chatelier's principle according to which an increase in the number of exchange sites covered by monovalent counterions favors the exchange to divalent counterions due to the reduction of the total molar concentration in the exchanger phase [27]. The preference for bivalent anions decreases with the distance between neighboring active sites on the AER (lower total exchange capacity) [26–28], which can explain why differences between sulphate and chloride were lower for PSR2Plus which has a lower total exchange capacity than the other two resins ( $\geq 0.7$  eq/L). Stronger inhibition of the adsorption of organic molecules on AERs resulting from divalent anions was also observed by Rahmani and Mohseni (2017) [45] and Tan et al. (2023) [54] who reported stronger inhibitory effects of sulphate compared to nitrate on the adsorption of different carboxylic acids and stronger inhibitory effects of sulphate and carbonate compared to hydrogen carbonate on the adsorption of PFASs to acrylic AERs, respectively. In contrast to the present study, neither of these previous studies tested [54] or observed [45] a decrease in adsorption capacity by inorganic anions for polystyrene-based AERs, which were used in the present study. This may be because the present study used higher inorganic anion concentrations ( $> 0.1$  mmol/L) and lower PFAA concentrations.

#### 4.2.2. Combined effects of sulphate and chloride

In previous studies on adsorption inhibition of PFASs onto AERs by inorganic anions, either only the impact of various single species was investigated [33,38,45–47], or combined effects were expressed as an equivalent background concentration (EBC) representing a matrix specific summarizing parameter which also includes NOM [31]. According to the authors' best knowledge, investigating combined effects of various single species in varying concentrations has not been conducted to date. In the batches with A111 and M600, the results show that, although charge equivalents were higher in the "both simultaneously" group than in the sulphate group, the adsorption inhibition was very similar. The assumption was statistically confirmed for A111, where no significant differences were found between the sulphate batches and the batches containing both anions for all PFAAs (Table A.6). At the same time, the adsorption inhibition of PFAAs in the mixture of both anions was well below the values predicted by the theoretical combined effect (dashed line). This shows that, in the presence of sulphate, the presence of additional chloride becomes more arbitrary for the PFAA adsorption and that adsorption inhibition was predominantly determined by the competitive effect of sulphate. This can be explained by the fact that chloride and sulphate also compete with each other for adsorption sites on the AERs, and the tested AERs preferred sulphate over chloride.

Contrary to A111 and M600, the combined effect of chloride and sulphate was greater than the effect of sulphate alone for PSR2Plus. In this case, the actual combined effect in the experimental series with both anions was comparable to the theoretical combined effect, which was also corroborated by significant differences between the experimental series with sulphate and both anions for the CF1–5 PFCAs. The relative effect of sulphate compared to chloride is therefore lower for PSR2Plus than for the other resins. This can be explained by the bulkier functional

groups of PSR2Plus compared to the other resins, resulting in greater distances between the neighboring functional groups and thus an increased selectivity for monovalent anions as mentioned in the previous section, which is indicated by its lower total exchange capacity of  $\geq 0.7$  eq/L [26–28]. By comparison, A111 and M600 had higher total exchange capacities of 1.7 eq/L and 1.3 eq/L and exhibit a higher preference for divalent anions due to less bulky functional groups. As PFAAs are also monovalent anions, the increased monoselectivity of PSR2Plus may also support an increased adsorption of the studied PFAAs and a lesser inhibition by inorganic anions.

#### 4.2.3. Effect of the resin functional group

The resins A111 and M600 performed similarly and there were no significant differences for the adsorption of PFPeA, PFHxA, PFOA and PFBS, and for all compounds in the experimental series with both chloride and sulphate ( $p > 0.05$ , Table A.7). In the batches with only chloride or sulphate, M600 performed slightly better than A111 ( $p < 0.05$ ) for the shorter chain PFAAs (CF1–3), particularly for the low inorganic anion concentration of 0.5 mmol/L. Despite almost 10-fold higher initial PFAA concentrations, equilibrium concentrations found in the batches with PSR2Plus were in the same range as for the other AERs (sheet "rawdata", column " $\gamma_{eq}$ ", Supplementary\_Information\_2.xlsx), implying a better adsorption performance and a lower susceptibility to the presence of inorganic anions. Previously, Zaggia et al. (2016) [34] found an increase in the selectivity towards PFASs with increasing alkyl chain lengths in the functional group and suggested a dependency on the hydrophobicity of the functional group. In the present study, there was an increase in the adsorption performance from A111 (dimethylamines) to M600 (dimethylethanolamines) to PSR2Plus (benzyltributylamines). As the number or length of alkyl moieties also increases in that order, this could also indicate the importance of hydrophobic interactions. This may still be true although the hydrophobicity of the functional group itself did not necessarily increase, since octanol-water distribution coefficients,  $\log D_{ow}$ , simulated with Percepta [55] for the respective functional group monomers at pH 7.0, were 0.94 for the (4-ethylphenyl)-N,N-dimethylmethanaminium (SMILES: C[NH+](C)Cc1ccc(cc1)CC) of A111,  $-2.46$  for the N-[(4-ethylphenyl)methyl]-2-hydroxy-N,N-dimethylethan-1-aminium (SMILES: C[N+](C)(Cc1ccc(cc1)CC)CCO) of M600, and 0.52 for the (4-ethylphenyl)-N,N,N-tributylmethanaminium (SMILES: CCCC[N+](CCCC)(Cc1ccc(cc1)CC)CCCC) of PSR2Plus. However, there are alternative explanations that involve differences in molecular charge density [56,57] or total atomic charge [58]. Park et al. (2020) [58] demonstrated that a negative charge interaction between PFAAs and functional resin groups can explain differences in the adsorption affinity of different PFAAs better than hydrophobic interactions by correlating the total negative atomic charge of PFAA molecules with the apparent equilibrium constants. The effect of differences in the total atomic charge of resin functional groups could thus be useful for a more detailed consideration for further work in this area but was outside the scope of the current study.

#### 4.2.4. Underlying correlation

A common approach for the estimation of the suitability of an adsorbent to treat a specific contaminant in a specific water matrix is to rely on documented case studies and scientific research that have been proven effective for similar water matrices and contaminants. However, the estimation becomes more difficult when there is no data available for comparable water matrices and accurate descriptions on how the treatment effectiveness correlates with the concentration of specific co-solutes. Regarding the effects of inorganic anions on the adsorption of PFAAs to AERs, previous studies have rarely included a range of different concentrations of respective anions [33,45–47], which would have allowed the derivation of a mathematical relationship to predict the adsorption effectiveness at varying anion concentrations.

In contrast, the present study investigated the adsorption of PFAAs at four different concentrations of sulphate and chloride. Hence, Eq. (3)

can be applied to test the double-logarithmic model to describe the relationship between  $\gamma/\gamma_0$  and the concentration of sulphate and chloride, respectively. Fig. 2 shows this correlation to be appropriate for the majority of the combinations of PFAAs and AERs. Table A.8 provides the statistical parameters for these correlations. The mathematical descriptions allow changes in the adsorption effectiveness to be quantified, enhancing the understanding of these relationships by progressing beyond mere qualitative statements. Furthermore, these findings can be linked to  $V_B$  values in fixed-bed filters according to Eqs. (5)–(10) and thus be used to make reasonable predictions of stoichiometric breakthroughs. Therefore, it was also shown that the logarithm of  $V_B$  is linearly correlated with the logarithm of  $c_{inorg,anion}$  (Section A.7). Fig. A.6 depicts the calculated linear isotherms (values for  $K$  are shown in the Supplementary\_Information\_2 on the sheet called “means”), while Fig. A.7 displays the double-logarithmic relationship between  $V_B$  and the inorganic ion concentrations. The statistical parameters for the single experimental batch groups and PFAA-AER-combinations are shown in Table A.9 and Table A.10. Examples of  $V_B$  predictions and a discussion about the implications for drinking water treatment using the tested AERs at specific chloride and sulphate concentrations is provided in Sections 4.4 and 4.5.

### 4.3. Dependence of adsorption inhibition on PFAA characteristics

Regardless of the AER used, adsorption was higher for PFSAs than for PFCAs with the same number of CF, i.e. TFMS vs. TFAA and PFBS vs. PFPeA, consistent with prior studies [16,25,34,35,59]. Adsorption also increased with longer chain PFAAs, while shorter chain PFAAs experienced stronger inhibition from sulphate and chloride. It should be noted

that previous studies also observed adsorption inhibition of shorter chain PFAAs by longer chain PFAAs [33]. Although initial PFAA concentrations were kept constant across all experimental groups in the present study, adsorption decreased with increasing chloride and sulphate concentrations (0–3.8 mmol/L). This suggests that inorganic anions, rather than inter-PFAA competition, primarily drove the adsorption inhibition. However, given the complex dynamics of adsorption processes, competitive interactions between different PFAAs cannot be entirely ruled out. The differences in the batches without inorganic anions, containing only demineralized water, may reflect the competitive effects by the longer chain PFAAs.

In all experimental series,  $\gamma/\gamma_0$  decreased logarithmically with CF, aligning with findings from soil and sediment adsorption studies [60, 61], as well as PFAA uptake in organisms [9,62] (Fig. 3). The regression slopes for PFCAs ranged from  $-0.25$  to  $-0.54$  log units per additional CF, with stronger effects seen at higher inorganic anion concentrations (see Table A.11 for regression parameters). This again indicates that shorter chain PFAAs were more influenced by  $c_{inorg,anion}$  changes than longer chain PFAAs, presumably due to factors such as their lower hydrophobicity, differences in charge density [56,57], and lower total negative atomic charge [58].

To provide context, Chow et al. (2022) reported similar trends for treated BVs as a function of PFCA chain length using PSR2Plus [63]. The chloride and sulphate concentrations in that study were between the concentrations used in the 0.5 mM and 1.3 mM treatment series containing both ions from the present study. Assuming a comparison of the  $\gamma/\gamma_0$ -CF-correlation with the BV-CF-correlation to be justifiable, the average slope found by Chow et al. ( $b_{avg} = 0.391$  log) was also between the slopes from the 0.5 mM ( $b_{avg} = -0.40$  log) and 1.3 mM ( $b_{avg} =$

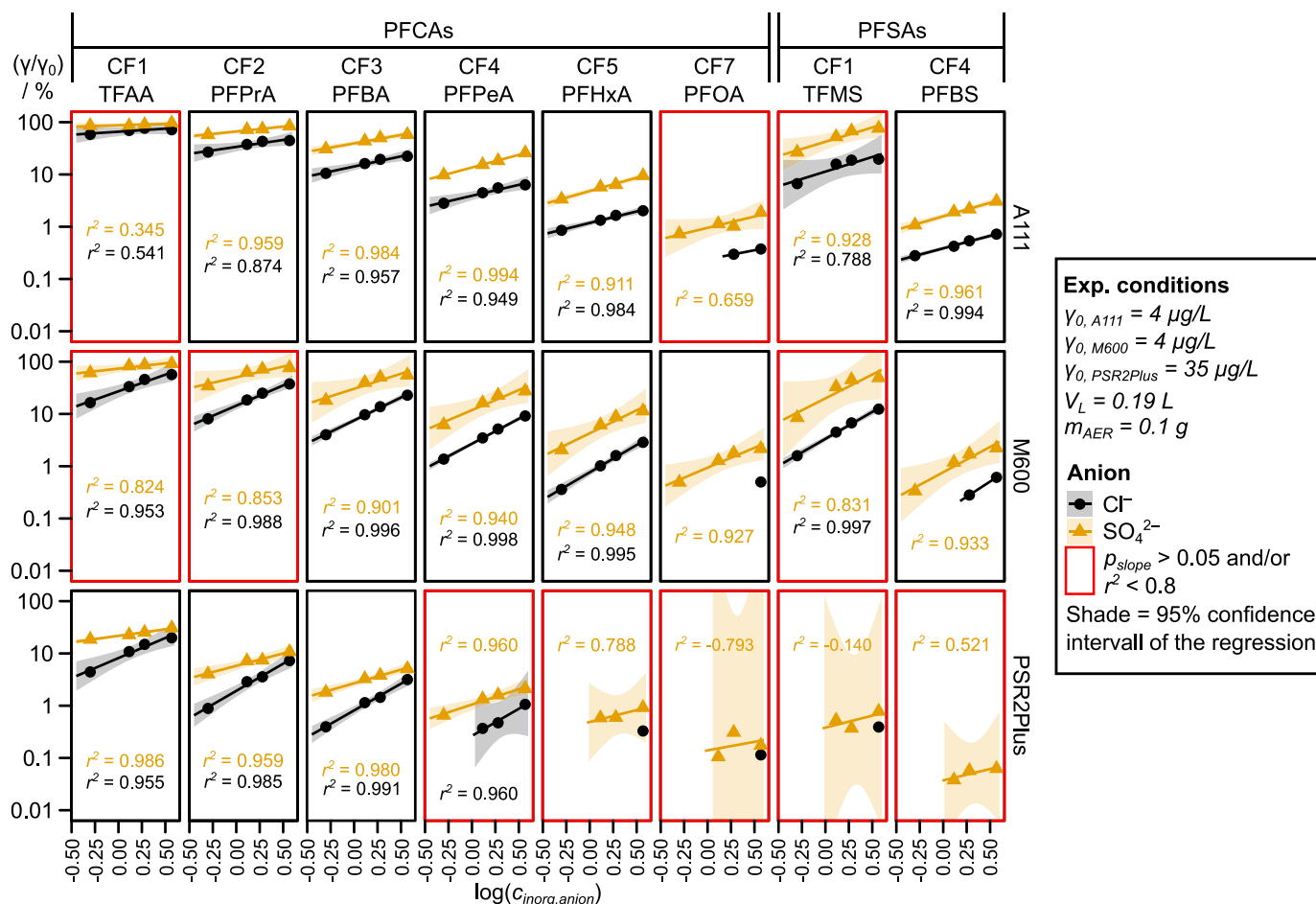


Fig. 2. Regression of the relative residual PFAA concentration,  $\gamma/\gamma_0$ , vs. chloride/sulphate concentration using three different AERs.

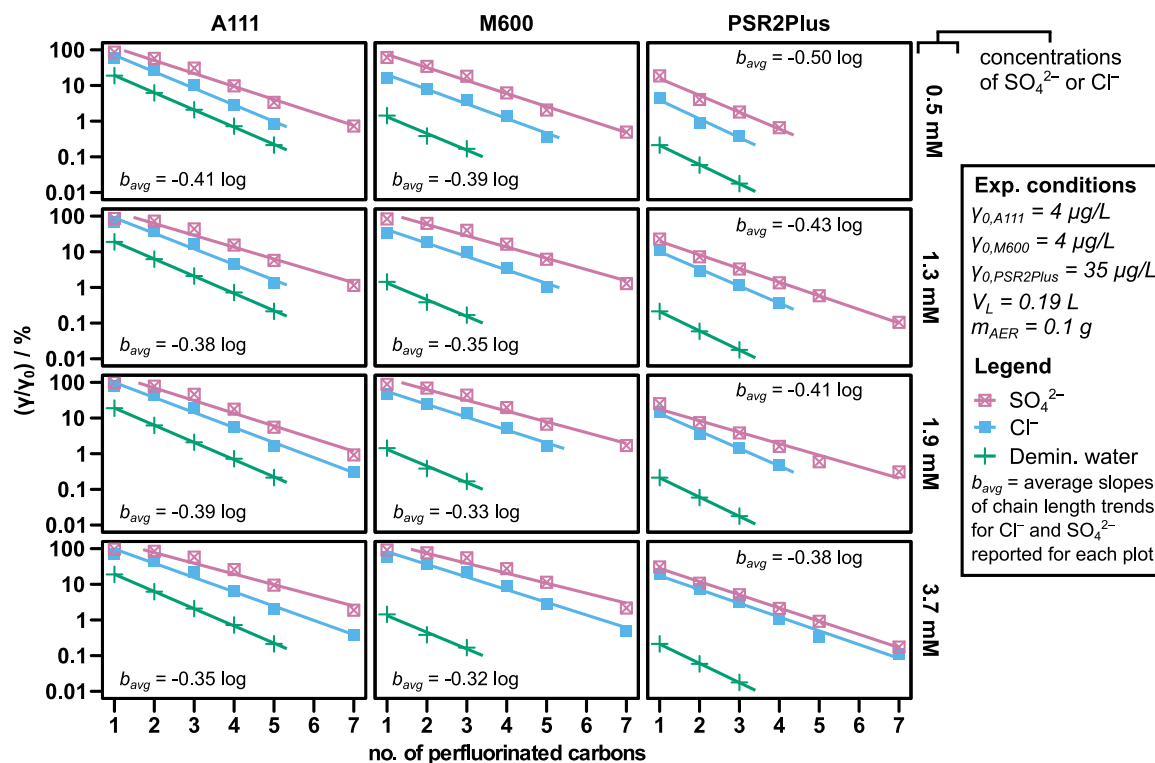


Fig. 3. Relative residual PFC concentration,  $\gamma/\gamma_0$ , vs. perfluorinated carbons at various sulphate/chloride concentrations using different AERs.

-0.35 log) groups with PSR2Plus [63]. The strong chain length correlation in  $\gamma/\gamma_0$  implies that the behavior of untested PFAAs in a homologous series can be inferred based on chain length in a given water matrix and include compounds that were not analyzed.

#### 4.4. A tool to estimate breakthroughs

Understanding how much water can be treated with an adsorbent before breakthroughs of target compounds occur is crucial for evaluating its operational and economic feasibility. The effectiveness of an adsorbent in one water matrix doesn't guarantee the same in another. To facilitate the selection of suitable adsorbents, this study aimed to provide a simple method of quantifying adsorption inhibition by relating it to specific concentrations of competing co-solutes, thus providing practitioners with a tool to estimate whether a given adsorbent remains viable in the presence of certain co-solute concentrations. This section discusses the precision and limitations regarding the prediction of  $V_B$  values from the chosen batch experimental approach.

It was assumed that predictions based on the concentration of the strongest inhibiting factor enhances the prediction accuracy. The dominant inhibitory effect of sulphate on the adsorption of PFAAs on A111 and M600, even in the presence of chloride, provided a good example of this. Therefore, Fig. 4 shows examples of  $V_B$  values for PFPPrA, PFBA, and PFPeA as a function of the sulphate concentration using A111, with calculated values derived from Eq. (8) and simulated values from the double logarithmic regression. Table 4 compares predicted  $V_B$  values at different sulphate concentrations for the three AERs, using PFBA as an example. More examples of calculated  $V_B$  values, including the other PFAAs and batch experimental series can be found in Section A.9.

Since no column experiments were conducted within the present study, calculated  $V_B$  were compared to 50 % breakthroughs reported in previous studies. Although a direct comparison was seldom possible due to differences in AERs, experimental designs and conditions, the comparison of  $V_B$  values and column breakthroughs for AERs with similar characteristics and similar sulphate concentrations showed a tendency

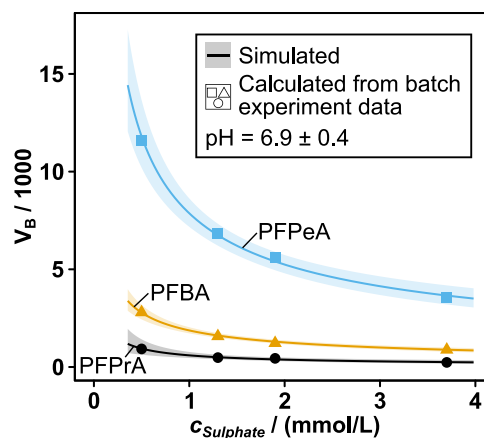


Fig. 4. Treated bed volumes prior to stoichiometric breakthrough,  $V_B$ , of short-chain PFCAs as a function of the sulphate concentration using A111. Equation for calculated values:  $V_B = K * \rho_F$ ; equation for simulated values:  $V_B = a * C_{inorg\ anion}^b$ .

for calculated  $V_B$  to overestimate actual breakthroughs. For example, Kassari et al. (2023) reported a 50 % breakthrough for PFBA in a column study after approximately 790 BV [42], using a weakly basic polystyrenic macroporous resin for the treatment of groundwater containing 48 mg/L sulphate, being considerably less than the calculated  $V_B$  from the present study with A111 at 50 mg/L sulphate (2700 BV). Similarly, calculated  $V_B$  for M600 (e. g. 4900 BV at 50 mg/L sulphate) also tend to overestimate the reported 50 % breakthroughs from column studies (700–5000 BV) [16,34,64] using AERs with comparable resin groups (type II and type I quaternary amines) and comparable or lower sulphate concentrations (0–44 mg/L). The same was observed when breakthroughs in previous column experiments using tri-n-butylamine AERs were compared to  $V_B$  values calculated for PSR2Plus in the experimental series with sulphate or both anions from the present study [25,65].



**Table 4**

Stoichiometric PFBA breakthroughs at different sulphate concentrations simulated for a fixed-bed filter with different AERs.

AER	$c_{\text{SO}_4^{2-}} / \text{mM}$	$\gamma_{\text{SO}_4^{2-}} / (\text{mg/L})$	$V_B$ (mean)	95 % ci	$t_B$ / days and 95 % ci
A111	0.52	50	2719	[2417; 3059]	11.3; [10.0; 12.7]
A111	1.25	120	1648	[1489; 1825]	6.9; [6.2; 7.6]
A111	3.85	370	866	[798; 939]	3.6; [3.3; 3.9]
M600	0.52	50	4914	[2195; 10999]	20; [9; 46]
M600	1.25	120	2258	[1124; 4533]	9.4; [4.7; 18.9]
M600	3.85	370	830	[476; 1450]	3.5; [2; 6]
PSR2Plus	0.52	50	64544	[28236; 147540]	269; [118; 615]
PSR2Plus	1.25	120	38623	[18889; 78975]	161; [79; 329]
PSR2Plus	3.85	370	19954	[11263; 35350]	83; [47; 147]

 $V_B$  = Stoichiometric breakthrough in bed volumes

ci = Confidence interval

 $t_B$  = Time until the stoichiometric breakthrough assuming a flow rate of 10 BV/h and 24-h-operation

These differences may occur because considering only sulphate as the likely dominant inhibitor may be an oversimplification and adsorption competition may also occur from unaccounted-for matrix compounds such as NOM [35,43–45] (with up to 2.2 mg/L [65]) and other common inorganic anions, e. g., hydrogen carbonate and nitrate (with up to 19 mg/L [34]). In addition, the results are only valid within the tested pH range at equilibrium ( $6.9 \pm 0.4$ ) for A111, because the capacity of weakly basic resins varies significantly with pH [38,41,46, 47,66]. Furthermore, previous studies have found that adsorption isotherm or equilibrium results alone cannot always precisely predict column performance under dynamic flow conditions due to mass transfer resistances, non-ideal equilibrium conditions, and axial dispersion in the column [27,53]. This is particularly true with GAC, because during the determination of equilibrium parameters, the GAC is typically ground, which creates additional adsorption sites and, in some cases, yields markedly different results than those obtained in columns utilizing the original granular activated carbon. For instance, Burkhardt et al. (2022) demonstrated that the Freundlich constants and kinetic rate constants of two types of GAC, F400 and AC1230CX, were nearly identical [67]. However, studies involving column experiments showed that F400 outperformed AC1230CX, despite the similarity in their isotherm data (e. g. [68]). Nevertheless, the analysis of ion exchangers does not entail grinding. Consequently, breakthrough predictions with equilibrium parameters are often more accurate for AERs [69,70]. Still, overestimations of the PFAS uptake by AERs in batch adsorption experiments in comparison with the adsorption in column studies have previously been shown [64].

For these reasons, the accuracy of the breakthroughs approximated by the presented method is limited. However, in accordance with the goal of the study, designing a method for initial estimates of  $V_B$  to compare different adsorbents, the results offer a quick pre-selection tool for adsorbents based on specific co-solute concentrations before conducting more elaborate fixed-bed filter experiments. Due to the likely overestimation of  $V_B$  values, the results can be interpreted as the best-case scenarios for water matrices containing the respective  $C_{\text{inorg.anion}}$ . Although column studies can provide more accurate and comprehensive information on dynamic adsorption, this approach can save time and resources for practitioners, such as drinking water suppliers, in the early stages of material evaluation. It offers an easy-to-apply evaluation

method to estimate the adsorption of PFAAs, or other pollutants, to adsorbents with various characteristics at a given concentration of a co-solute. The tool also allows for a basic assessment of cost effectiveness so that an AER can be excluded from consideration early on, if it is shown to be economically unfeasible. Moreover, the concrete results from this study can be directly applied (serve as first estimates) when AERs with the same or similar polymer composition, functional groups, and exchange capacities are used for PFAA adsorption in drinking water containing sulphate and chloride in the tested concentration range (0.5–3.8 mmol/L), and low amounts of other co-solutes such as NOM.

Nevertheless, in terms of a holistic material evaluation, it is suggested to use the data obtained by the presented method as a basis for further investigations with pre-selected adsorbents. For example, the knowledge gained could be used in combination with dynamic column studies or other models such as the Langmuir or Freundlich isotherm to improve the accuracy of results. Linking the shaking tests with rapid small scale column results could provide a useful approach to optimize cost and time while improving accuracy.

#### 4.5. Usability of the tested AERs for drinking water treatment

Economic viability depends on the point at which the filter material needs to be replaced, which is influenced by the composition of the water matrix and the treatment objective. For instance, if the treatment objective is to meet the EU drinking water directive's sum of PFAS threshold of 0.1  $\mu\text{g/L}$  [11], the presence or absence of short-chain PFCAs in relevant concentrations can significantly impact the suitability of an AER due to their shorter  $t_B$  compared to longer chain PFCAs and PFSAs (Table A.12–16). For instance, estimated  $V_B$  values for PFOA and PFBS were between 69000 BV and 134000 BV, even at 120 mg/L sulphate, making the tested AERs suitable candidates for further investigation. However, if the exchange of the filter material were defined by the breakthrough of PFBA instead, the  $V_B$  values in Table 4 are very low in comparison, with mean  $V_B$  for PSR2Plus being between 20000 BV and 65000 BV. For A111 and M600, the  $V_B$  values for PFBA at presumed sulphate concentrations between 50 mg/L and 370 mg/L were below 5000 BV. Consequently, the AERs would require replacement at high frequency with fresh material, if they were to be used as single-use adsorbents that are not reused following a regeneration process.

An effective and cost-efficient regeneration procedure could greatly enhance the total runtime of an AER and increase its economic viability [36,71,72]. In this regard, the weakly basic resin A111 could have an advantage over the two strongly basic resins, as regeneration of AERs loaded with PFASs is typically easier for weakly basic resins [23,42]. Because the results show that A111 can effectively remove PFAAs in its free base form, presumably no change of the form would be required after regeneration with a caustic solution. Effects of a potential extension of the operation time through regeneration and a proper comparison with runtimes from single-use operation cannot be determined with the presented method. However, the use of weakly basic AERs for PFAS treatment requires further research as only a few studies have investigated the continuous use of weakly basic AERs in consecutive adsorption and regeneration cycles [71,73].

## 5. Conclusion

This study contributes to an enhanced understanding of PFAS adsorption onto AERs by elucidating correlations of adsorption with influential factors such as the functional resin groups, PFAA chain length and functional group, and the competitive effects of sulphate and chloride. Moreover, the study demonstrates how insights derived from batch experiments can inform first estimations of fixed-bed filter operation through the use of a simple model. The correlations determined here and the stoichiometric breakthrough can serve as a tool and foundational framework for an informed selection of AERs when planning further research on fixed-bed filters, potentially streamlining

experimental efforts by leveraging the information presented herein.

## Funding

This project has received funding from the European Union's Horizon 2020 research and innovation program under grant agreement No. 101036756.

## CRedit authorship contribution statement

**Lukas Lesmeister:** Writing – original draft, Visualization, Validation, Methodology, Investigation, Conceptualization. **Sarah E. Hale:** Writing – review & editing, Funding acquisition. **Michael Merklinger:** Writing – review & editing, Resources. **Harald Horn:** Writing – review & editing, Conceptualization. **Marcel Riegel:** Writing – review & editing, Supervision, Project administration.

## Declaration of Competing Interest

The authors declare that they have no known competing financial interests or personal relationships that could have appeared to influence the work reported in this paper.

## Acknowledgements

The authors thank Alina Schlosser, Ralph Schäfer, and Sibylla Nordwig-Krauß for their support with the laboratory work. This project has received funding from the European Union's Horizon 2020 research and innovation program under grant agreement No. 101036756.

## Appendix A. Supporting information

Supplementary data associated with this article can be found in the online version at [doi:10.1016/j.jece.2024.114871](https://doi.org/10.1016/j.jece.2024.114871).

## Data availability

Data will be made available on request.

## References

- [1] R.C. Buck, J. Franklin, U. Berger, J.M. Conder, I.T. Cousins, P. de Voogt, A. Jensen, K. Kannan, S.A. Mabury, S.P.J. van Leeuwen, Perfluoroalkyl and polyfluoroalkyl substances in the environment: Terminology, classification, and origins, *Integr. Environ. Assess. Manag.* 7 (2011) 513–541, <https://doi.org/10.1016/10.1002/ieam.258>.
- [2] S. Snitsiriwat, J.M. Hudzik, K. Chaisaward, L.R. Stoler, J.W. Bozzelli, Thermodynamic properties: enthalpy, entropy, heat capacity, and bond energies of fluorinated carboxylic acids, *J. Phys. Chem. A* 126 (2022) 3–15, <https://doi.org/10.1016/10.1021/acs.jpca.1c05484>.
- [3] H. Lee, S.A. Mabury, Global distribution of polyfluoroalkyl and perfluoroalkyl substances and their transformation products in environmental solids, in: D. A. Lambropoulou, L.M.L. Nolle (Eds.), *Transformation products of emerging contaminants in the environment: Analysis, processes, occurrence, effects and risks*, Wiley, Chichester, 2014, pp. 797–825.
- [4] K.A. Barzen-Hanson, S.C. Roberts, S. Choyke, K. Oetjen, A. McAlees, N. Riddell, R. McCrindle, P.L. Ferguson, C.P. Higgins, J.A. Field, Discovery of 40 Classes of Per- and Polyfluoroalkyl Substances in Historical Aqueous Film-Forming Foams (AFFFs) and AFFF-Impacted Groundwater, *Environ. Sci. Technol.* 51 (2017) 2047–2057, <https://doi.org/10.1016/10.1021/acs.est.6b05843>.
- [5] I.J. Neuwald, D. Hübner, H.L. Wiegand, V. Valkov, U. Borchers, K. Nödler, M. Scheurer, S.E. Hale, H.P.H. Arp, D. Zahn, Ultra-short-chain PFASs in the sources of German drinking water: prevalent, overlooked, difficult to remove, and unregulated, *Environ. Sci. Technol.* 56 (2022) 6380–6390, <https://doi.org/10.1016/10.1021/acs.est.1c07949>.
- [6] I.T. Cousins, C.A. Ng, Z. Wang, M. Scheringer, Why is high persistence alone a major cause of concern? *Environ. Sci. Process. Impacts* 21 (2019) 781–792, <https://doi.org/10.1016/10.1039/c8em00515j>.
- [7] I.T. Cousins, J.C. DeWitt, J. Glüge, G. Goldenman, D. Herzke, R. Lohmann, C.A. Ng, M. Scheringer, Z. Wang, The high persistence of PFAS is sufficient for their management as a chemical class, *Environ. Sci. Process. Impacts* 22 (2020) 2307–2312, <https://doi.org/10.1016/10.1039/d0em00355g>.
- [8] M. Scheurer, K. Nödler, F. Freeling, J. Janda, O. Happel, M. Riegel, U. Müller, F. R. Storck, M. Fleig, F.T. Lange, A. Brunsch, H.-J. Brauch, Small, mobile, persistent: Trifluoroacetate in the water cycle - Overlooked sources, pathways, and consequences for drinking water supply, *Water Res.* 126 (2017) 460–471, <https://doi.org/10.1016/j.watres.2017.09.045>.
- [9] L. Lesmeister, F.T. Lange, J. Breuer, A. Biegel-Engler, E. Giese, M. Scheurer, Extending the knowledge about PFAS bioaccumulation factors for agricultural plants - A review, *Sci. Total Environ.* 766 (2021) 142640, <https://doi.org/10.1016/j.scitotenv.2020.142640>.
- [10] P.A. Behnisch, H. Besselink, R. Weber, W. Willand, J. Huang, A. Brouwer, Developing potency factors for thyroid hormone disruption by PFASs using TTR-TR $\beta$  CALUX<sup>®</sup> bioassay and assessment of PFASs mixtures in technical products, *Environ. Int.* 157 (2021) 106791, <https://doi.org/10.1016/j.envint.2021.106791>.
- [11] Directive (EU) 2020/2184 of the European parliament and the council of 16 December 2020 on the quality of water intended for human consumption: EU 2020/2184.
- [12] OECD, Toward a new comprehensive global database of per- and polyfluoroalkyl substances (PFASs): Summary Report on updating the OECD 2007 List of per- and polyfluoroalkyl substances (PFASs).
- [13] B.C. Crone, T.F. Speth, D.G. Wahman, S.J. Smith, G. Abulikemu, E.J. Kleiner, J. G. Pressman, Occurrence of Per- and Polyfluoroalkyl Substances (PFAS) in Source Water and Their Treatment in Drinking Water, *Crit. Rev. Environ. Sci. Technol.* 49 (2019) 2359–2396, <https://doi.org/10.1016/10.1080/10643389.2019.1614848>.
- [14] I. Ross, J. McDonough, J. Miles, P. Storch, P. Thelakatt Kochunarayanan, E. Kalve, J. Hurst, S.S. Dasgupta, J. Burdick, A review of emerging technologies for remediation of PFASs, *Remediat. J.* 28 (2018) 101–126, <https://doi.org/10.1016/10.1002/rem.21553>.
- [15] M. Park, S. Wu, I.J. Lopez, J.Y. Chang, T. Karanfil, S.A. Snyder, Adsorption of perfluoroalkyl substances (PFAS) in groundwater by granular activated carbons: Roles of hydrophobicity of PFAS and carbon characteristics, *Water Res.* 170 (2020) 115364, <https://doi.org/10.1016/j.watres.2019.115364>.
- [16] P. McCleaf, S. Englund, A. Östlund, K. Lindegren, K. Wiberg, L. Ahrens, Removal efficiency of multiple poly- and perfluoroalkyl substances (PFASs) in drinking water using granular activated carbon (GAC) and anion exchange (AE) column tests, *Water Res.* 120 (2017) 77–87, <https://doi.org/10.1016/j.watres.2017.04.057>.
- [17] R. Mukhopadhyay, B. Sarkar, K.N. Palansooriya, J.Y. Dar, N.S. Bolan, S.J. Parikh, C. Sonne, Y.S. Ok, Natural and engineered clays and clay minerals for the removal of poly- and perfluoroalkyl substances from water: State-of-the-art and future perspectives, *Adv. Colloid Interface Sci.* 297 (2021) 102537, <https://doi.org/10.1016/j.cis.2021.102537>.
- [18] I.M. Militao, F. Roddick, L. Fan, L.C. Zepeda, R. Parthasarathy, R. Bergamasco, PFAS removal from water by adsorption with alginate-encapsulated plant albumin and rice straw-derived biochar, *J. Water Process Eng.* 53 (2023) 103616, <https://doi.org/10.1016/j.jwpe.2023.103616>.
- [19] P. Das, V.A. Arias E, V. Kambala, M. Mallavarapu, R. Naidu, Remediation of perfluorooctane sulfonate in contaminated soils by modified clay adsorbent—a risk-based approach, *Water Air Soil Pollut.* 224 (2013) 1326, <https://doi.org/10.1016/10.1007/s11270-013-1714-y>.
- [20] R. Medina, M.W. Pannu, S.A. Grieco, M. Hwang, C. Pham, M.H. Plumlee, Pilot-scale comparison of granular activated carbons, ion exchange, and alternative adsorbents for per- and polyfluoroalkyl substances removal, *AWWA Water Sci.* 4 (2022) 107, <https://doi.org/10.1016/10.1002/aww2.1308>.
- [21] J. Szabo, J. Hall, M. Magnuson, S. Panguluri, G. Meiners, Treatment of Perfluorinated Alkyl Substances in Wash Water Using Granular Activated Carbon and Mixed-Media.
- [22] J. Wang, Z.-W. Lin, W.R. Dichtel, D.E. Helbling, Perfluoroalkyl acid adsorption by styrenic  $\beta$ -cyclodextrin polymers, anion-exchange resins, and activated carbon is inhibited by matrix constituents in different ways, *Water Res.* 260 (2024) 121897, <https://doi.org/10.1016/j.watres.2024.121897>.
- [23] T.H. Boyer, Y. Fang, A. Ellis, R. Dietz, Y.J. Choi, C.E. Schaefer, C.P. Higgins, T. J. Strathmann, Anion exchange resin removal of per- and polyfluoroalkyl substances (PFAS) from impacted water: A critical review, *Water Res.* 200 (2021) 117244, <https://doi.org/10.1016/j.watres.2021.117244>.
- [24] F. Dixit, R. Dutta, B. Barbeau, P. Berube, M. Mohseni, PFAS removal by ion exchange resins: A review, *Chemosphere* 272 (2021) 129777, <https://doi.org/10.1016/j.chemosphere.2021.129777>.
- [25] A.C. Ellis, C.J. Liu, Y. Fang, T.H. Boyer, C.E. Schaefer, C.P. Higgins, T. J. Strathmann, Pilot study comparison of regenerable and emerging single-use anion exchange resins for treatment of groundwater contaminated by per- and polyfluoroalkyl substances (PFASs), *Water Res.* 223 (2022) 119019, <https://doi.org/10.1016/j.watres.2022.119019>.
- [26] A.K. Sengupta, *Ion Exchange Technology: Advances in Pollution Control*, Technomic Pub, Lancaster, PA, 1995.
- [27] A.K. Sengupta, *Hoboken, NJ. Ion Exchange in Environmental Processes*, 1st ed., Wiley, 2017.
- [28] K. Dorfner, *Ion Exchangers*, Walter de Gruyter, Berlin, 1991.
- [29] K.-U. Goss, The pKa values of PFOA and other highly fluorinated carboxylic acids, *Environ. Sci. Technol.* 42 (2008) 456–458, <https://doi.org/10.1016/10.1021/es702192c>.
- [30] T.M.H. Nguyen, J. Bräunig, K. Thompson, J. Thompson, S. Kabiri, D.A. Navarro, R. S. Kookana, C. Grimison, C.M. Barnes, C.P. Higgins, M.J. McLaughlin, J.F. Mueller, Influences of Chemical Properties, Soil Properties, and Solution pH on Soil-Water Partitioning Coefficients of Per- and Polyfluoroalkyl Substances (PFASs), *Environ. Sci. Technol.* 54 (2020) 15883–15892, <https://doi.org/10.1016/10.1021/acs.est.0c05705>.

- [31] F. Dixit, B. Barbeau, K.M. Lompe, A. Kheyrandish, M. Mohseni, Performance of the HSDM to predict competitive uptake of PFAS, NOM and inorganic anions by suspended ion exchange processes, *Environ. Sci.: Water Res. Technol.* 7 (2021) 1417–1429, <https://doi.org/10.1016/10.1039/D1EW00145K>.
- [32] F. Dixit, B. Barbeau, S.G. Mostafavi, M. Mohseni, PFOA and PFOS removal by ion exchange for water reuse and drinking applications: Role of organic matter characteristics, *Environ. Sci.: Water Res. Technol.* 5 (2019) 1782–1795, <https://doi.org/10.1016/10.1039/c9ew00409b>.
- [33] A. Maimaiti, S. Deng, P. Meng, W. Wang, B. Wang, J. Huang, Y. Wang, G. Yu, Competitive adsorption of perfluoroalkyl substances on anion exchange resins in simulated AFFF-impacted groundwater, *Chem. Eng. J.* 348 (2018) 494–502, <https://doi.org/10.1016/j.cej.2018.05.006>.
- [34] A. Zaggia, L. Conte, L. Falletti, M. Fant, A. Chiorboli, Use of strong anion exchange resins for the removal of perfluoroalkylated substances from contaminated drinking water in batch and continuous pilot plants, *Water Res.* 91 (2016) 137–146, <https://doi.org/10.1016/j.watres.2015.12.039>.
- [35] L.L. del Moral, Y.J. Choi, T.H. Boyer, Comparative removal of Suwannee River natural organic matter and perfluoroalkyl acids by anion exchange: Impact of polymer composition and mobile counterion, *Water Res.* 178 (2020) 1–9, <https://doi.org/10.1016/j.watres.2020.115846>.
- [36] H. Smaili, C. Ng, Adsorption as a remediation technology for short-chain per- and polyfluoroalkyl substances (PFAS) from water – a critical review, *Environ. Sci.: Water Res. Technol.* 9 (2023) 344–362, <https://doi.org/10.1016/10.1039/D2EW00721E>.
- [37] P. Li, A.K. Sengupta, Genesis of selectivity and reversibility for sorption of synthetic aromatic anions onto polymeric sorbents, *Environ. Sci. Technol.* 32 (1998) 3756–3766, <https://doi.org/10.1016/10.1021/es980628y>.
- [38] Y. Gao, S. Deng, Z. Du, K. Liu, G. Yu, Adsorptive removal of emerging polyfluoroalkyl substances P-53B and PFOS by anion-exchange resin: A comparative study, *J. Hazard. Mater.* 323 (2017) 550–557, <https://doi.org/10.1016/j.jhazmat.2016.04.069>.
- [39] L.-A.M.B. Dudley, Removal of Perfluorinated Compounds by Powdered Activated Carbon, Superfine Powdered Activated Carbon, and Anion Exchange Resins. Master Thesis, Raleigh, North Carolina, 2012.
- [40] M.F. Rahman, W.B. Anderson, S. Peldszus, P.M. Huck, Ion-exchange treatment of perfluorinated carboxylic acids in water: comparison of polystyrenic and polyacrylic resin structures and impact of sulfate on their performance, *ACS EST Water* 2 (2022) 1195–1205, <https://doi.org/10.1016/10.1021/acestwater.1c00501>.
- [41] C. Kassir, C. Graham, T.H. Boyer, Removal of perfluoroalkyl acids and common drinking water contaminants by weak-base anion exchange resins: Impacts of solution pH and resin properties, *Water Res.* X 17 (2022) 100159, <https://doi.org/10.1016/j.wroa.2022.100159>.
- [42] C. Kassir, T.H. Boyer, Removal of PFAS from groundwater using weak-base anion exchange resins, *AWWA Water Sci.* 5 (2023), <https://doi.org/10.1016/10.1002/aww2.1325>.
- [43] D.N. Kothawala, S.J. Köhler, A. Östlund, K. Wiberg, L. Ahrens, Influence of dissolved organic matter concentration and composition on the removal efficiency of perfluoroalkyl substances (PFASs) during drinking water treatment, *Water Res.* 121 (2017) 320–328, <https://doi.org/10.1016/j.watres.2017.05.047>.
- [44] F. Dixit, B. Barbeau, S.G. Mostafavi, M. Mohseni, PFAS and DOM removal using an organic scavenger and PFAS-specific resin: Trade-off between regeneration and faster kinetics, *Sci. Total Environ.* 754 (2021) 142107, <https://doi.org/10.1016/j.scitotenv.2020.142107>.
- [45] H.-M. Tan, C.-G. Pan, C. Yin, K. Yu, Insights into the Understanding of Adsorption Behaviors of Legacy and Emerging Per- and Polyfluoroalkyl Substances (PFASs) on Various Anion-Exchange Resins, *Toxics* 11 (2023), <https://doi.org/10.1016/10.3390/toxics11020161>.
- [46] Y. Yang, Q. Ding, M. Yang, Y. Wang, N. Liu, X. Zhang, Magnetic ion exchange resin for effective removal of perfluoroctanoate from water: Study of a response surface methodology and adsorption performances, *Environ. Sci. Pollut. Res. Int.* 25 (2018) 29267–29278, <https://doi.org/10.1016/10.1007/s11356-018-2797-1>.
- [47] S. Deng, Q. Yu, J. Huang, G. Yu, Removal of perfluoroctane sulfonate from wastewater by anion exchange resins: Effects of resin properties and solution chemistry, *Water Res.* 44 (2010) 5188–5195, <https://doi.org/10.1016/j.watres.2010.06.038>.
- [48] L. Lesmeister, M. Riegel, N. Zumbülte, N. Löffler, F.T. Lange, Deliverable 7.1: Ad-/desorption performance of IEX resins towards short chain PFAA. Work Package 7 – Technical Solutions, Method Development and Analysis. ([https://zeropm.eu/wp-content/uploads/2023/03/Deliverable\\_7.1\\_final.pdf](https://zeropm.eu/wp-content/uploads/2023/03/Deliverable_7.1_final.pdf)) (accessed March 12, 2024).
- [49] E. Gagliano, M. Sgroi, P.P. Falciglia, F.G.A. Vagliasindi, P. Roccaro, Removal of poly- and perfluoroalkyl substances (PFAS) from water by adsorption: Role of PFAS chain length, effect of organic matter and challenges in adsorbent regeneration, *Water Res.* 171 (2020) 115381, <https://doi.org/10.1016/j.watres.2019.115381>.
- [50] DIN 32645, 11, 2008, Chemical analysis - Decision limit, detection limit and determination limit under repeatability conditions - Terms, methods, evaluation, Beuth Verlag GmbH, Berlin, 2008. (<https://www.beuth.de/de/norm/din-32645/110729574>) (accessed January 29, 2024).
- [51] DIN EN ISO 10304-1:2009-07, 2009, Water quality - Determination of dissolved anions by liquid chromatography of ions - Part 1: Determination of bromide, chloride, fluoride, nitrate, nitrite, phosphate and sulfate (ISO 10304-1:2007); German version EN ISO 10304-1:2009, Beuth Verlag GmbH, Berlin. <https://dx.doi.org/10.31030/1518948>.
- [52] R Core Team, R: The R Project for Statistical Computing (Version 4.2.2), R Foundation for Statistical Computing, Vienna, Austria, 2022.
- [53] H. Sontheimer, B.R. Frick, J. Fetting, G. Hörner, C. Hubele, G. Zimmer, Adsorptionsverfahren zur Wasserreinigung, DVGW-Forschungsstelle am Engler-Bunte-Institut der Universität Karlsruhe, Karlsruhe, 1985.
- [54] S. Rahmani, M. Mohseni, The role of hydrophobic properties in ion exchange removal of organic compounds from water, *Can. J. Chem. Eng.* 95 (2017) 1449–1455, <https://doi.org/10.1016/10.1002/cjce.22823>.
- [55] ACD/Labs, Percepta: GALAS model (Version 2.3), Toronto, Ontario, Canada, 2022.
- [56] F. Dixit, B. Barbeau, S.G. Mostafavi, M. Mohseni, Efficient removal of GenX (HFPPO-DA) and other perfluorinated ether acids from drinking and recycled waters using anion exchange resins, *J. Hazard. Mater.* 384 (2020) 121261, <https://doi.org/10.1016/j.jhazmat.2019.121261>.
- [57] B.A. Parker, D.R.U. Knappe, I.A. Titaley, T.A. Wanzek, J.A. Field, Tools for Understanding and Predicting the Affinity of Per- and Polyfluoroalkyl Substances for Anion-Exchange Sorbents, *Environ. Sci. Technol.* 56 (2022) 15470–15477, <https://doi.org/10.1016/10.1021/acs.est.1c08345>.
- [58] M. Park, K.D. Daniels, S. Wu, A.D. Ziska, S.A. Snyder, Magnetic ion-exchange (MIEX) resin for perfluorinated alkylsubstance (PFAS) removal in groundwater: Roles of atomic charges for adsorption, *Water Res.* 181 (2020) 115897, <https://doi.org/10.1016/j.watres.2020.115897>.
- [59] M. Ateia, M. Arifuzzaman, S. Pellizzeri, M.F. Attia, N. Tharayil, J.N. Anker, T. Karanfil, Cationic polymer for selective removal of GenX and short-chain PFAS from surface waters and wastewaters at ng/L levels, *Water Res.* 163 (2019) 114874, <https://doi.org/10.1016/j.watres.2019.114874>.
- [60] C.P. Higgins, R.G. Luthy, Sorption of perfluorinated surfactants on sediments, *Environ. Sci. Technol.* 40 (2006) 7251–7256, <https://doi.org/10.1016/10.1021/es061000n>.
- [61] J.L. Guelfo, C.P. Higgins, Subsurface transport potential of perfluoroalkyl acids at aqueous film-forming foam (AFFF)-impacted sites, *Environ. Sci. Technol.* 47 (2013) 4164–4171, <https://doi.org/10.1016/10.1021/es3048043>.
- [62] S. Zhao, S. Fang, L. Zhu, L. Liu, Z. Liu, Y. Zhang, Mutual impacts of wheat (*Triticum aestivum* L.) and earthworms (*Eisenia fetida*) on the bioavailability of perfluoroalkyl substances (PFASs) in soil, *Environ. Pollut.* 184 (2014) 495–501, <https://doi.org/10.1016/j.envpol.2013.09.032>.
- [63] S.J. Chow, H.C. Croll, N. Ojeda, J. Klamerus, R. Capelle, J. Oppenheimer, J. G. Jacangelo, K.J. Schwab, C. Prasse, Comparative investigation of PFAS adsorption onto activated carbon and anion exchange resins during long-term operation of a pilot treatment plant, *Water Res.* 226 (2022) 119198, <https://doi.org/10.1016/j.watres.2022.119198>.
- [64] B. Liu, Y.-L. Liu, M. Sun, Remove legacy perfluoroalkyl acids and emerging per- and polyfluoroalkyl ether acids by single-use and regenerable anion exchange resins: Rapid small-scale column tests and model fits, *Water Res.* 257 (2024) 121661, <https://doi.org/10.1016/j.watres.2024.121661>.
- [65] L. Cheng, D.R.U. Knappe, Removal of Per- and Polyfluoroalkyl substances by anion exchange resins: Scale-up of rapid small-scale column test data, *Water Res.* 249 (2024) 120956, <https://doi.org/10.1016/j.watres.2023.120956>.
- [66] W. Wang, A. Maimaiti, H. Shi, R. Wu, R. Wang, Z. Li, D. Qi, G. Yu, S. Deng, Adsorption behavior and mechanism of emerging perfluoro-2-propoxypropanoic acid (GenX) on activated carbons and resins, *Chem. Eng. J.* 364 (2019) 132–138, <https://doi.org/10.1016/j.cej.2019.01.153>.
- [67] J.B. Burkhardt, N. Burns, D. Mobley, J.G. Pressman, M.L. Magnuson, T.F. Speth, Modeling PFAS Removal Using Granular Activated Carbon for Full-Scale System Design, *J. Environ. Eng. (N. Y., N. Y.)* 148 (2022) 1–11, [https://doi.org/10.1061/\(ASCE\)EE.1943-7870.0001964](https://doi.org/10.1061/(ASCE)EE.1943-7870.0001964).
- [68] M.W. Pannu, J. Chang, R. Medina, S.A. Grieco, M. Hwang, M.H. Plumlee, Comparing PFAS removal across multiple groundwaters for eight GACs and alternative adsorbent, *AWWA Water Sci.* 5 (2023) 11728, <https://doi.org/10.1016/10.1002/aww2.1345>.
- [69] J. Janda, F.T. Lange, M. Riegel, Weitergehende Erfassung von PFC-Quellen im Einzugsbereich von Wasserwerken und Entfernung von kurzkettigen, persistenten PFC: Abschlussbericht. W 07-03-14.
- [70] M. Riegel, Untersuchungen zur Elimination von natürlichen Uranspezies aus Wässern mit Hilfe schwach basischer Anionenaustauscher, Dissertation, Karlsruhe, 2009.
- [71] M. Riegel, B. Haist-Gulde, F. Sacher, Sorptive removal of short-chain perfluoroalkyl substances (PFAS) during drinking water treatment using activated carbon and anion exchanger, *Environ. Sci. Eur.* 35 (2023) 266, <https://doi.org/10.1016/10.1186/s12302-023-00716-5>.
- [72] I. Emery, D. Kempisty, B. Fain, E. Mbonimpa, Evaluation of treatment options for well water contaminated with perfluorinated alkyl substances using life cycle assessment, *Int J. Life Cycle Assess.* 24 (2019) 117–128, <https://doi.org/10.1016/10.1007/s11367-018-1499-8>.
- [73] M. Riegel, Entfernung (kurzkettiger) PFAS mit einem neuen Ansatz aus Aktivkohle und Ionenaustauscher, Vom Wasser 120 (2022) 4–9, <https://doi.org/10.1016/10.1002/vomw.202200001>.